Full Paper

CONTRAST MEDIA & MOLECULAR IMAGING

Received: 30 March 2013, Revised: 10 September 2013, Accepted: 23 September 2013, Published online in Wiley Online Library

(wileyonlinelibrary.com) DOI: 10.1002/cmmi.1574

Gd loading by hypotonic swelling: an efficient and safe route for cellular labeling

Enza Di Gregorio, Giuseppe Ferrauto, Eliana Gianolio and Silvio Aime*

Cells incubated in hypo-osmotic media swell and their membranes become leaky. The flow of water that enters the cells results in the net transport of molecules present in the incubation medium directly into the cell cytoplasm. This phenomenon has been exploited to label cells with MRI Gd-containing contrast agents. It has been found that, in the presence of 100 mM Gd–HPDO3A in an incubation medium characterized by an overall osmolarity of 160 mOsm l^{-1}, each cell is loaded with amounts of paramagnetic complex ranging from 2×10^9 to 2×10^{10} depending on the cell type. To obtain more insight into the determinants of cellular labeling by the 'hypo-osmotic shock' methodology, a study on cell viability, proliferation rate and cell morphology was carried out on J774A.1 and K562 cells as representative of cells grown in adhesion and suspended ones, respectively. Moreover a comparison of the efficiency of the proposed method with established cell labeling procedures such as pinocytosis and electroporation was carried out. Finally, the effects of the residual electric charge, the size and some structural features of the metal complex were investigated. In summary, the 'hypotonic shock' methodology appears to be an efficient and promising tool to pursue cellular labeling with paramagnetic complexes. Its implementation is straightforward and one may foresee that it will be largely applied in *in vitro* cellular labeling of many cell types. Copyright © 2013 John Wiley & Sons, Ltd.

Additional supporting information may be found in the online version of this article at the publisher's web site.

Keywords: Gd-complex; MRI; hypotonic swelling; cell labeling; Paramagnetic complexes

1. INTRODUCTION

The development of strategies for cellular labeling is of great interest for *in vivo* cell tracking in the emerging field of cell therapy for regenerative medicine. Among the available imaging modalities, magnetic resonance imaging (MRI) appears to be the candidate of choice for its high spatial resolution, the absence of ionizing radiation and the unlimited penetration of radiofrequencies in biological tissues (1–4). *Ex-vivo* cellular labeling procedures for ^{1}H-MRI detection are mainly based on the use of superparamagnetic particles acting on T_2 and T_2* (5–9) or Gd complexes acting on T_1 (10–14). Recently, paraCEST agents have also been considered as labeling agents because their frequency-encoding properties allow the simultaneous visualization of different cell populations in the same anatomical region (15–17). In general the use of (ultrasmall) paramagnetic iron oxide particles (SPIO/USPIO) is advantageous in terms of sensitivity with respect to T_1 and CEST agents, but the fact that they act by reducing the intensity of signal may be considered a drawback because it may be confused with other sources of hypointense signal (e.g. tissue interfaces, air or motion artifacts, tissues/organs with intrinsic low signal like lungs or regions characterized by short T_2). For this reason, the use of 'positive' gadolinium-based contrast agents, acting on T_1 of 'bulk' water protons, is still under intense scrutiny. In order to be visualized by MRI, a cell has to be loaded with large amounts of Gd complexes.

The issue of the minimum amount of Gd(III) complexes necessary to allow the MRI visualization of cells has been tackled by several authors (18,19). In a review work of 2002 (12), we made an in-depth analysis of the previous findings in this field, and reported our results on hepatotropic Gd complexes internalized into hepatocytes. By imaging pellets of ca. 5 millions of cells, we drew the conclusion that, for contrast agent endowed with relaxivities in the range of 4–7 mM^{-1} s^{-1}, the minimum amount of Gd(III) units per cell necessary for the attainment of enough contrast in an MR image is about 2×10^9. Five million pelleted cells roughly correspond to a volume of 10–20 μl, which means around $1.2–2.5 \times 10^8$ cell ml^{-1}. Typical cell densities values for tissues are close to this number, being in the range of $1.5–3 \times 10^8$ cell ml^{-1}.

Different routes for the internalization of Gd complexes into cells have been explored (20–22), including macropinocytosis, electroporation and receptor/transporter-mediated endocytosis. According to the used methodology, the paramagnetic agents are localized in the cytoplasm or in the endosomes. When large amounts of paramagnetic compounds are confined in endosomal vesicles (i.e. of the order of 10^9 per cell or more), a dramatic decrease of T_2^* and a 'quenching' of the attainable T_1 enhancement in the corresponding MR images occurs. In particular, the T_1 'quenching' takes place when the difference in the relaxation rates between endosomes and cytoplasm is higher than the exchange rate between the two compartments, that is, $|R_1^{end} - R_1^{cyt}| > \text{or} >> k_{ex}^{cyt\text{-}end}$ (14,23–25). For this reason, it is sometimes advantageous to use the electroporation route that

* *Correspondence to: S. Aime, Molecular Imaging Center, Department of Molecular Biotechnologies and Health Sciences, University of Torino, Via Nizza 52, 10126-Torino, Italy. Email: silvio.aime@unito.it*

E. Di Gregorio, G. Ferrauto, E. Gianolio, S. Aime
Molecular Imaging Center, Department of Molecular Biotechnologies and Health Sciences, University of Torino, Via Nizza 52, 10126- Torino, Italy

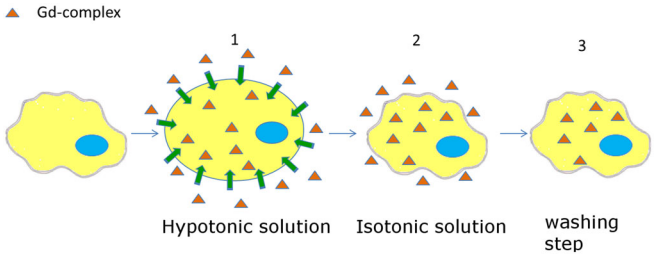

Figure 1. Key-step of the hypotonic swelling method for cellular labeling: (1) cells placed into a hypotonic solution containing the MRI contrast agents (extracellular environment, ca. 130–200 mOsm l^{-1}; intracellular space, 280 mOsm l^{-1}) swell and the cytoplasmatic membrane becomes permeable to labeling agents; (2) the external medium is brought to an isotonic osmolarity and the morphology of cells is restored; and (3) non-internalized molecules are removed by successive washing.

leads to the entrapment of the labeling agents into the cytoplasmatic compartment. This loading procedure is often used for loading drugs, nucleic acids, etc., even though it is well known that it is always accompanied by severe drawbacks such as changes in cell morphology, cell viability and proliferation rate (26–30).

Herein we report results obtained by labeling cells via the exploitation of effects associated with the induction of an 'osmotic shock'. This method exploits temporary de-structuring events occurring at the cellular membrane in the presence of osmotic gradients between the intracellular and the extracellular compartments. In particular, when the osmotic pressure of the extracellular compartment is lower than that of the intracellular one, the net result is the swelling of the cells as a consequence of the incoming of water molecules into the inner cellular space. During swelling, the membrane is less efficient in acting as a

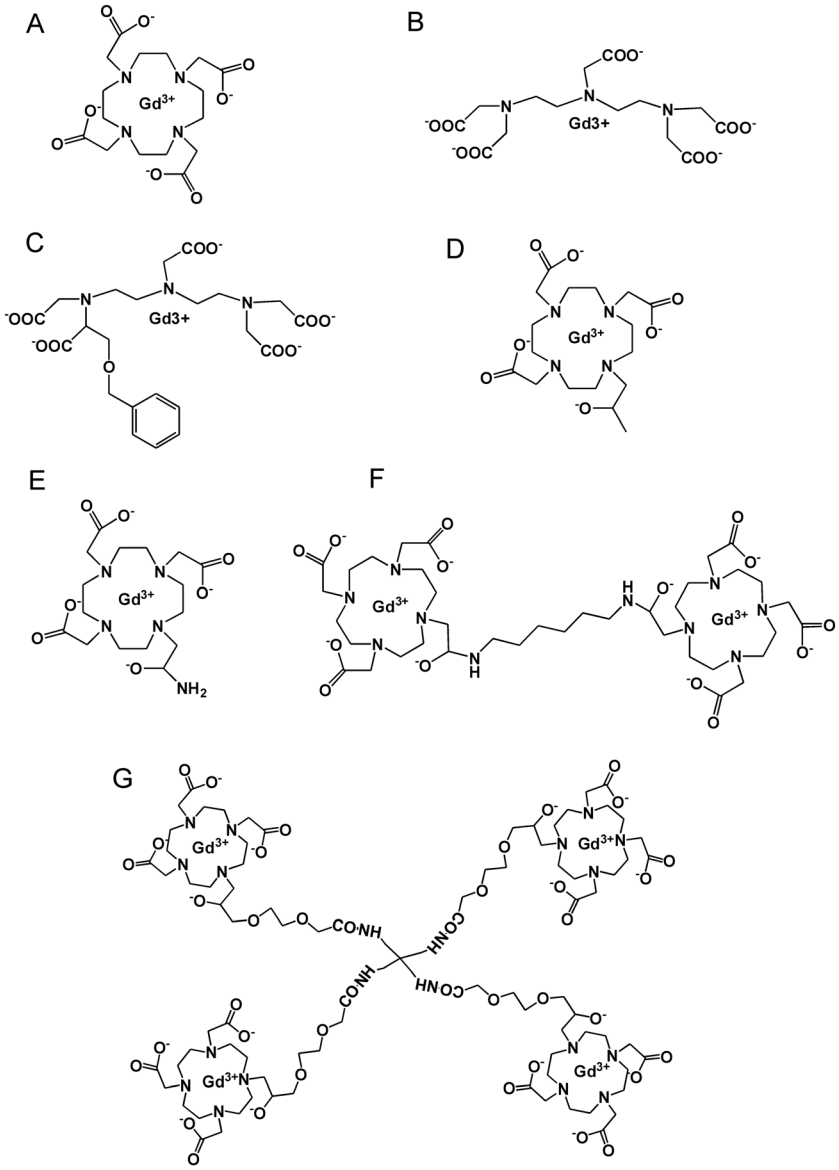

Scheme 1. Molecular structures of the Gd complexes used for cellular labeling: (A) Gd–DOTA (Dotarem®), (B) Gd–DTPA (Gadopentetate dimeglumine, Magnevist®), (C) Gd–BOPTA (Gadobenate dimeglumine, MultiHance®), (D) Gd–HPDO3A (Gadoteridol, ProHance®, Bracco), (E) Gd–HPDO3A-NH_2, (F) dimer of Gd–HPDO3A and (G) tetramer of Gd–HPDO3A.

barrier to the molecular transits, thus molecules can be relatively free to cross the 'temporarily injured' membranes.

In spite of the general acceptance that the cell swelling upon hypo-osmotic shock causes partial loss of membrane integrity, there is not yet a good explanation for the observed behavior. Actually, the microscopic steps that are at the basis of the swelling mechanism have not been completely elucidated. It has been suggested that caveolae (characteristic plasma membrane invaginations) have a role as a physiological membrane reservoir that quickly accommodates the mechanical stresses (31). In fact caveolae flattening is likely to release the amount of membrane stored within the caveolar invagination and then to provide the additional membrane required to maintain membrane tension homeostasis during mechanical stress. It was also suggested that the plasma membrane's expansion may result from the selective fusion with numerous small vesicles present in the cytoplasm (32). Furthermore it is well accepted that cell swelling brings about changes in the cytoskeleton following exposure to hypotonic medium (33,34). Of course, when the osmotic stress is too intense or it lasts for a long time, cells activate programmed cell death apoptosis.

An increase in membrane permeability upon exposure to hypotonic solution was assessed by propidium iodide DNA staining methodology in carp spermatozoa (35). As the rate of propidium iodide uptake increased with decreasing osmotic pressure, it was not clear if it was due to a continuously growing population of highly permeabilized cells.

In the field of cellular labeling for MR applications, the hypo-osmotic shock method has been used by Magnani et al. for labeling red blood cells with iron-oxide particles (36–38). Furthermore, an early report (39) dealing with the application of the method for the labeling of red blood cells with Gd–DOTA was not followed by dedicated applications. Herein we show that the advantages observed in the labeling of RBC may be translated to a number of cell types, thus enabling the method with a quite general applicability.

2. RESULTS AND DISCUSSION

As shown in Fig. 1, the method relies on the effects associated to the osmotic shock that is produced by suspending eukaryotic cells into a hypo-osmotic solution containing the molecules that have to be internalized into the cells (step 1, Fig. 1). Under the osmotic pressure, the cells swell, increasing their size and membrane permeability. During this phase the molecules of interest enter the cells moved by the concentration gradient. At the end of this phase, cell shape and morphology can be restored simply by returning the osmolarity of the extracellular solution to an iso-osmotic condition (step 2, Fig. 1). Not internalized molecules are then removed by successive washings with phosphate-buffered saline (PBS; step 3, Fig 1).

Gadoteridol (Gd–HPDO3A, Scheme 1), an MRI detectable probe, has been used to optimize the conditions for cell labeling. This molecule is a common MRI contrast agent normally used as an extracellular agent but it has been reported, in preclinical studies, also as a cellular label for MRI detection because it is small-sized, hydrophilic, neutral and normally well tolerated by the cell machinery also at high intracellular concentrations (16).

2.1. Evaluation of Membrane Resealing After the Application of Hypotonic Swelling Procedure

The cellular membrane resealing time after the application of hypotonic swelling treatment has been evaluated for J774A.1 cells by using the Methylene Blue staining method (Fig. 2). The dye normally does not cross cell membranes so the observation of blue cells is taken as an indication of altered membrane permeability. The number of Methylene Blue-positive cells decreases by increasing the delay time from the starting of resealing step to the addition of the Blue dye. When Methylene Blue was added during the last 5 min of the swelling step (i.e. before the resealing step operated by restoring the iso-osmolar conditions) the amount of blue cells was 40%. Conversely, when Methylene Blue was added simultaneously ($t = 0$) or after increasing times during the resealing process, the number of blue-colored cells decreased markedly (from ca. 6% at $t = 0$ to ca. 3% at $t \geq 15$ min). The dotted lines indicate the number of blue cells observed upon incubation with Methylene Blue for 5 min in the absence of any swelling phenomenon (i.e. probably the result of pinocytosis uptake or owing to apoptotic cells with reduced membrane integrity). The observed behavior is indicative of a relatively fast membrane resealing after the swelling step, as in ca. 10–15 min the membrane permeability appears completely restored.

2.2. Major Determinants of Hypotonic Swelling Cell Labeling Procedure

In order to identify the major determinants for the proposed internalization procedure, the work has been carried out on murine macrophages (J774A.1) and human leukemia cells (K562). These two cell types have been chosen as representative of cells that grow in adhesion on the culture plate or in suspension, respectively.

For both cell types, the amounts of Gd-loaded molecules per cell, upon the application of hypotonic swelling, have been assessed and results are reported in Fig. 3. It was found that, under the applied experimental conditions, the amount of Gd^{3+} per cell was in the order of 10^{10}, that is, well above the threshold for cell visualization by MRI. Gadolinium intracellular

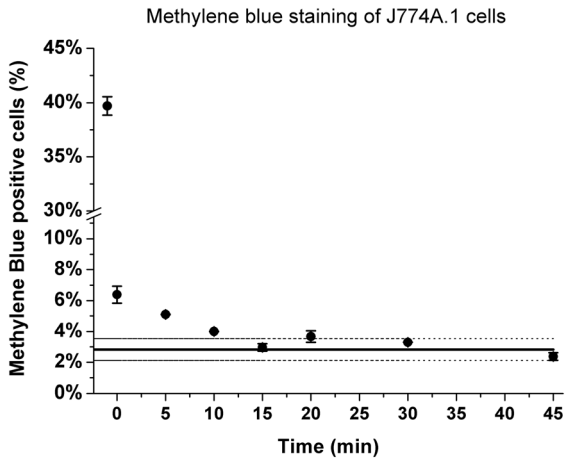

Figure 2. Resealing of cells membranes after the application of hypotonic swelling. Dotted lines indicate the percentage of cells that internalize Methylene Blue without the application of the osmotic treatment.

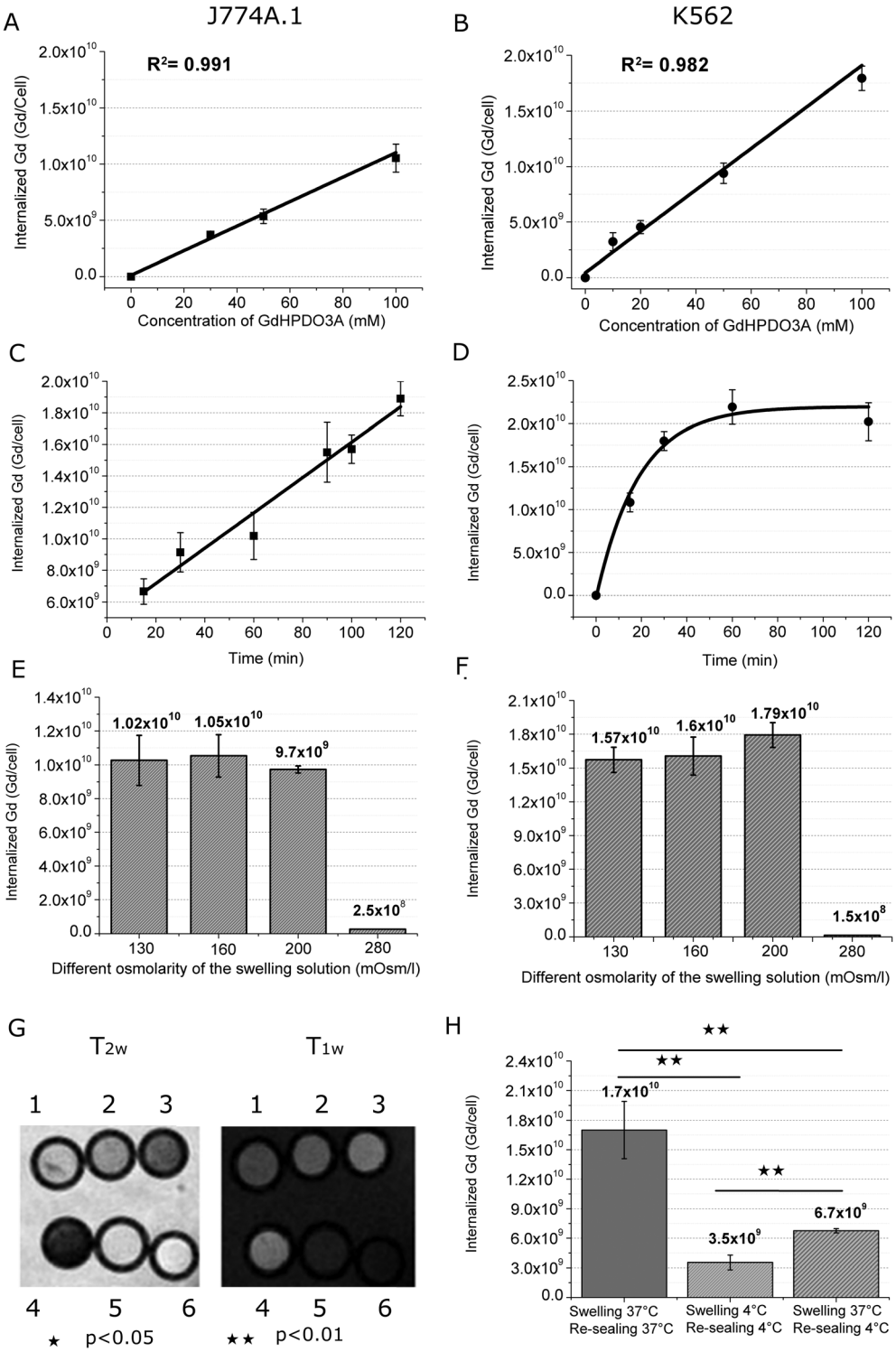

Figure 3. Amounts of internalized Gd–HPDO3A per cell for J774A.1 (left) and K562 (right) cells by applying the hypotonic swelling methodology as a function of the Gd complex concentration in the external solution (A, B) or of the labeling time (C, D) or of the hypotonic solution osmolarity (E, F). (G) T_{2w} and T_{1w} MR images of a phantom containing Gd–HPDO3A labeled-J774A.1 cellular pellets. The phantom contains the following samples: (1–4) cells having undergone the 'osmotic-shock' labeling procedure in the presence of increasing concentrations of Gd–HPDO3A in the hypotonic medium (30, 50, 70 or 100 mM); (5) unlabeled J774A.1 cells; (6) water. (H) Amount of internalized Gd–HPDO3A per cell for K562 cells by changing the temperature of swelling and/or resealing steps. All data in the graphs are reported as mean values ± standard deviation of at least three independent experiments.

concentrations of 10–20 mM were reached when [Gd] in the bathing solutions was of the order of 100 mM. This one order of magnitude deficit between intra- and extracellular concentrations is the result of a complex interplay among a number of structural and dynamic effects. During cellular swelling, the structure of the membrane loses, in part, its integrity, allowing exchange of materials between the extra- and intracellular compartments. Obviously, loss of intracellular substances has

an effect on the cell viability. Fortunately, the hypotonic swelling procedure results in a very favorable balance between good uptake of Gd complexes from the external compartment and the overall cell viability.

By varying the concentration of Gd–HPDO3A in the hypotonic medium, a linear increase of the internalized Gd complex per cell was observed (Fig. 3A and B). As expected, this increase corresponds to an increase in the signal intensity in a T_1-weighted MR image and a decrease in the corresponding T_2-weighted image. Figure 3(G) shows representative T_{1w} and T_{2w} images of pellets of J774A.1 cells labeled with increasing concentrations (30,50,70,100 mM – capillaries 1–4) of Gd–HPDO3A using an incubation time of 30 min and an osmolarity of 160 mOsm l^{-1} compared with unlabeled cells (capillary 5) and water (capillary 6). Hyperintense signals are observed in the T_{1W} image for the pellets containing labeled cells with respect to the unlabeled ones. A 126% signal enhancement with respect to control cells was obtained even in the case of cells labeled with the lower concentration of Gd–HPDO3A (ca. 3×10^9 Gd per cell).

Next, other determinants of the cell loading efficiency for the hypo-osmotic shock methodology were assessed. In Fig. 3(C and D) results obtained by changing the time during which the cells were maintained in hypotonic conditions are reported. The amount of internalized Gd complexes per cell increased with the incubation time for both K562 and for J774A.1 cells even if, for K562 cells, a plateau was reached when the amount of internalized complex was ca. 2×10^{10} Gd per cell.

By changing the osmolarity of the incubation solution in the range of 130–200 mOsm l^{-1}, no significant change in the amounts of the internalized Gd complex was observed (Fig. 3E and F). In contrast, marked temperature dependence was observed. In Fig. 3(H) the amounts of Gd–HPDO3A internalized into K562 cells (30 min of hypotonic swelling, 100 mM of GdHPDO3A, incubation medium 160 mOsm l^{-1}) upon changing the experimental temperature are reported. In the first experiment, both swelling and resealing were carried out at 37 °C; in the second experiment, both steps were performed at 4 °C and in the third experiment, the swelling was carried out at 37 °C and the resealing at 4 °C. The obtained results clearly show that the highest efficiency of internalization was obtained when the entire experiment was carried out at 37 °C.

2.3. Comparison with Pinocytosis and Electroporation Labeling Procedures

The ability of K562 and J774A.1 cells to uptake Gd–HPDO3A by hypotonic swelling has been compared with the loadings attainable by pinocytosis and electroporation (Fig. 4). Macrophages (J774A.1) have a high capability to internalize molecules through macropinocytosis, so this route is undoubtedly the preferred one for this cell type as far as the loading efficiency is concerned. In contrast, for K562, pinocytosis is less efficient and the number of internalized Gd complexes is ca. half those taken up by means of the hypotonic swelling method. Electroporation for both cell types appears to lead to a higher internalization when compared with the hypotonic swelling (Fig. 4A and B for J774A.1 and K562, respectively).

As a control experiment, the amount of internalized Gd–HPDO3A by simple incubation of cells for 30 min in an isotonic medium containing the Gd complex at 100 mM concentration at 37 °C was measured. The amount of internalized Gd–HPDO3A was ca. two order of magnitude lower (2.5×10^8 and 1.5×10^8 Gd per cell for J774A.1 and K562 cells, respectively) than that obtained when the uptake experiment was carried out in a hypotonic medium.

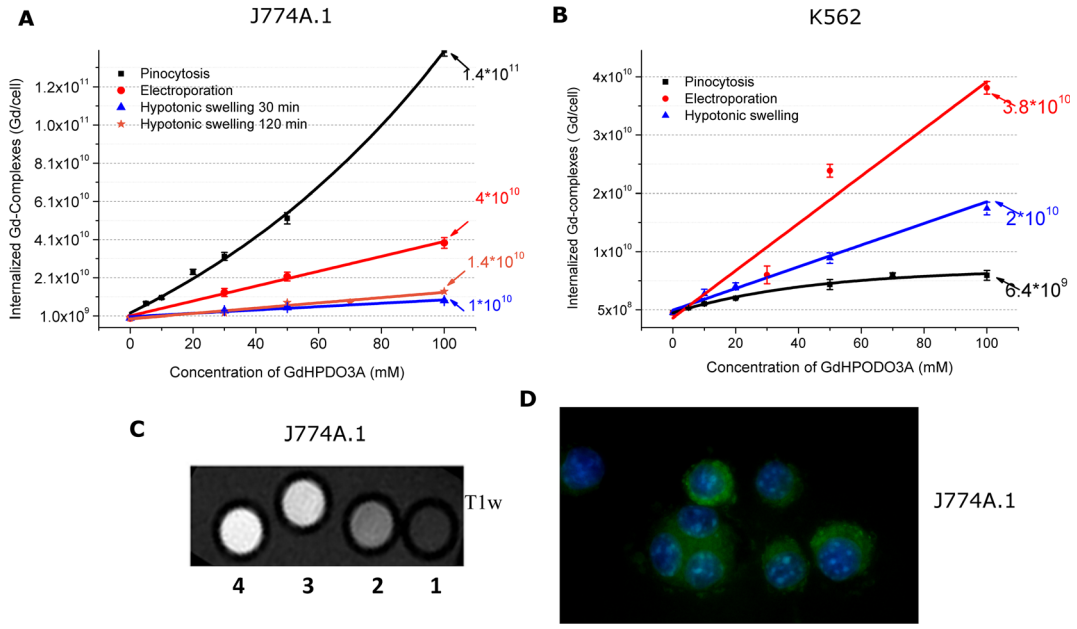

Figure 4. Comparison between the application of pinocytosis, electroporation and hypotonic swelling (30 min, 160 mOsm l^{-1}) to internalize Gd–HPDO3A at different concentrations in the incubation medium. (A) J774A.1 and (B) K562 cells. In the case of pinocytosis J774A.1 and K562 cells were incubated at 37 °C for 5 and 18 h, respectively. The intracellular localization of the probes loaded by hypotonic swelling was evaluated by MRI and microscopy. (C) T_{1w} MR image of a phantom containing J774A.1 cellular pellets: (1) unlabeled J774A.1 cells; (2) J774A.1 cells labeled with Gd–HPDO3A by pinocytosis (1.39×10^{10} Gd per cell); (3) by electroporation (1.49×10^{10} Gd per cell); and (4) by hypotonic swelling (1.33×10^{10} Gd per cell). (D) Fluorescence image of J774A.1 cells labeled by hypotonic swelling in the presence of 0.5 mM carboxyfluorescein. Nuclei were stained using Hoechst 33342 dye.

A comparison of the imaging capabilities attainable by the three labeling procedures, that is, pinocytosis, electroporation and hypotonic swelling, on J774A.1 cells labeled with Gd–HPDO3A, was then pursued (Fig. 4C). The T_1 contrast observed for pellets of cells labeled by means of the hypotonic swelling procedure was similar to that observed for cells labeled by electroporation (Fig. 4C, capillary 4 vs capillary 3). In contrast (Fig. 4C, capillary 2), by exploiting the pinocytosis route, the typical 'quenching' of relaxivity was observed (r_{1p} results were 2.1, 4.2 and 4.3 $mM^{-1}s^{-1}$ for pinocytosis, electroporation and hypotonic swelling, respectively). This result clearly reflects the different intracellular localization of the paramagnetic probe in the case of pinocytosis or hypotonic swelling/electroporation methods. The intra-cytoplasmatic compartmentalization of the probe in the cells labeled by the hypo-osmotic swelling method was confirmed by adding CarboxyFluorescein to the incubation medium. A representative image showing a clear spread-out of the probe in the cell cytosol is shown in Fig. 4(D).

Moreover, a comparison between the three labeling procedures was carried out also in terms of cell viability and functionality. The percentage of viable cells upon the application of the hypotonic swelling procedure was significantly higher than that obtained by applying electroporation (ca. 90 vs 65%) and only slightly lower than that attained by exploiting the spontaneous cellular pinocytosis (Fig. 5A). On going from experiments carried out in a neat buffer to solutions containing 100 mM Gd–HPDO3A, a nonsignificant ($p > 0.12$) decrease in the cell viability (5–6%) was observed either for electroporation or for 'osmotic shock' procedures. Concerning the proliferation rate (Fig. 5B), it was found that this parameter was only slightly modified upon hypotonic swelling treatment or pinocytosis with respect to control. Conversely, by applying electroporation, a marked decrease in the proliferation rate was observed.

More insights into cells viability issue have been acquired by evaluating the amount of apoptotic cells and reactive oxygen species (ROS) production. In Fig. 5(C) the amounts of apoptotic cells found 24 and 48 h after the labeling treatments are reported. In the cases of pinocytosis and hypotonic swelling, only a small number of cells had undergone apoptosis at 24 and 48 h after the labeling step. In contrast, in the case of electroporation, high levels of apoptotic cells were found, especially in the first few hours following the labeling step.

Finally, the production of ROS upon the application of the labeling procedures was evaluated (Fig. 5D). While electroporation led to a marked increase in ROS production in respect to the control cells, the hypotonic swelling method triggered only a small increase in production of ROS.

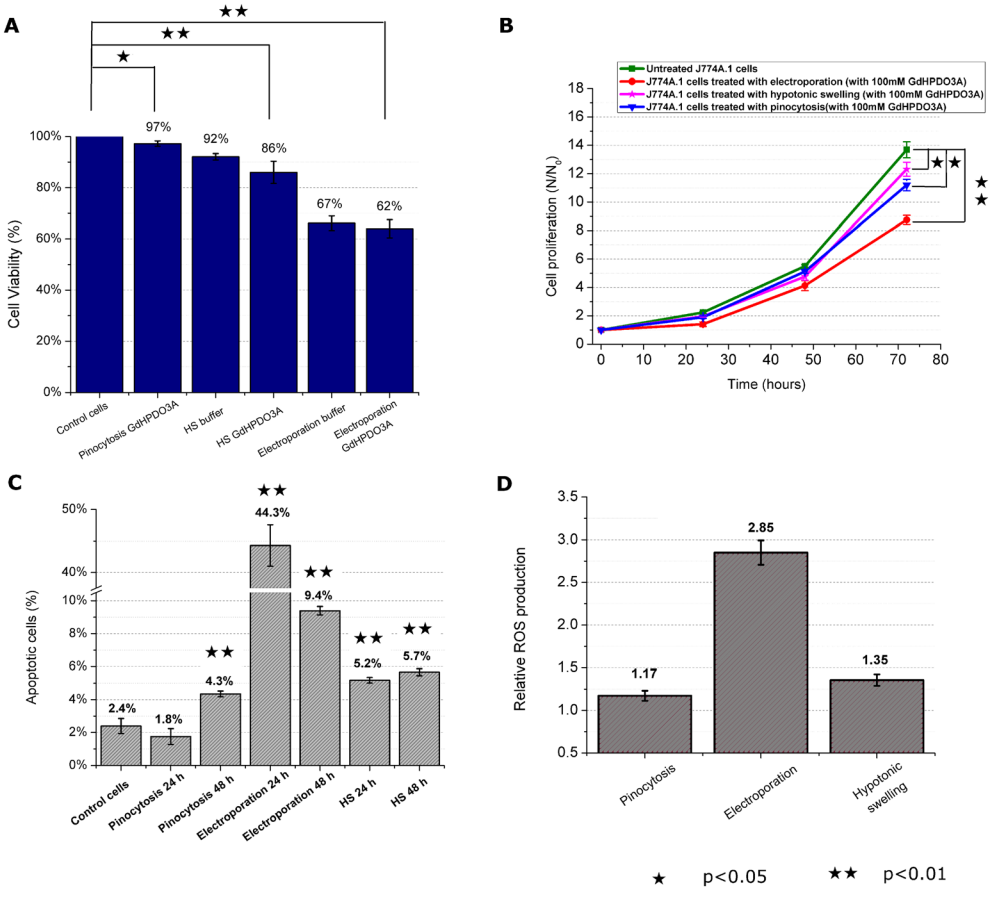

Figure 5. Cell viability (A) and proliferation (B) assays for J774A.1 cells after pinocytosis, electroporation or hypotonic swelling (with Gd–HPDO3A 100 mM or buffer). (C) Evaluation of the number of apoptotic cells at 24 or 48 h after application of pinocytosis, electroporation or hypotonic swelling. (D) Relative reactive oxygen species production in J774A.1 cells after application of pinocytosis, electroporation or hypotonic swelling. All data in the graphs are reported as mean values ± standard deviation of at least three independent experiments.

Overall, among the three cell labeling procedures, electroporation was invariantly the most aggressive one in terms of the observed results for cell viability, proliferation rate, apoptosis and ROS production. Conversely, the hypotonic swelling procedure seems to be endowed with a considerably higher level of biocompatibility, comparable to that shown by the pinocytotic internalization route.

Table 1. Pros and cons of the main cellular labeling procedures with MRI contrast agents

	Pinocytosis	Electroporation	Hypotonic swelling
Required time	Long, depending on cell type (1–24 h)	Short (1 h)	Short (1–2 h)
Amount of internalized Gd probes	High for macrophages Low for other cells	High	Medium/high
Cell viability	High	Low	High
Change in proliferation rate	Negligible	Significant/marked	Negligible
Cellular localization of the internalized molecules and related problems	Inside endosomes/phagosomes • The more aggressive endosomal/lysosomal compartments may cause extensive degradation of the entrapped contrast agent molecules • The MRI efficiency may be limited by the relaxivity 'quenching'	Cytoplasmatic • The less aggressive cytoplasmatic compartment appears to maintain the structural integrity of the entrapped contrast agent molecules	Cytoplasmatic • The less aggressive cytoplasmatic compartment appears to maintain the structural integrity of the entrapped contrast agent molecules

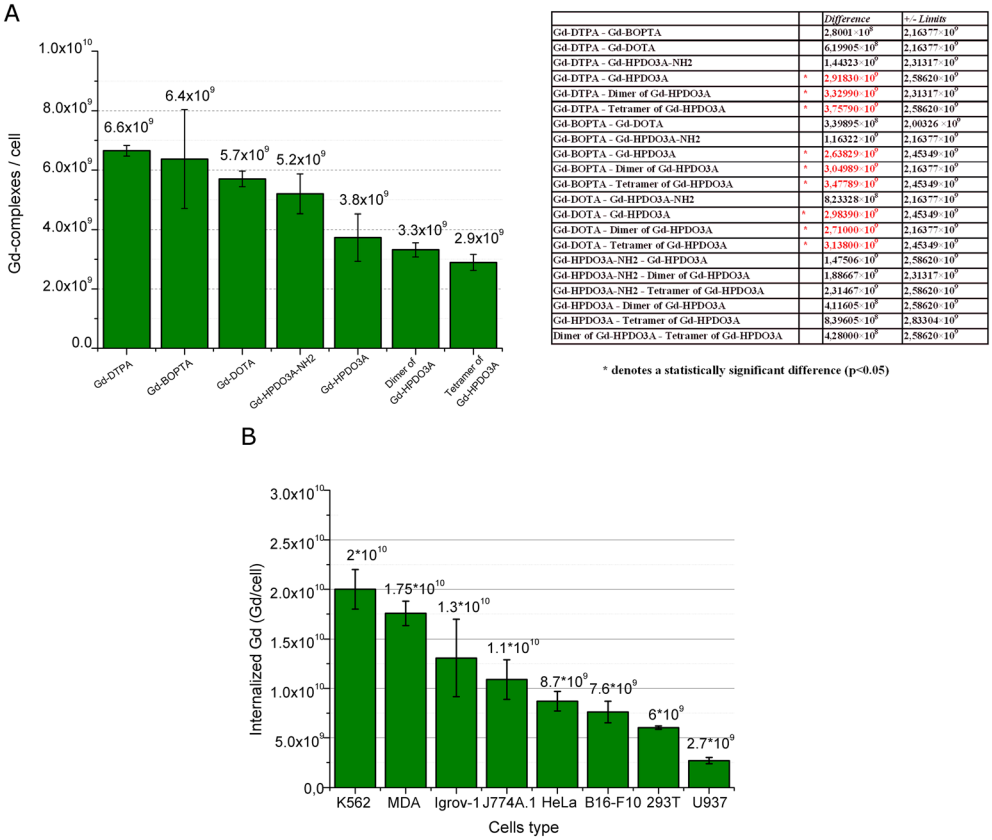

		Difference	+/- Limits
Gd-DTPA - Gd-BOPTA		2.8001·10^9	2.1637·10^9
Gd-DTPA - Gd-DOTA		6.19905·10^9	2.1637·10^9
Gd-DTPA - Gd-HPDO3A-NH2		1.44323·10^9	2.31317·10^9
Gd-DTPA - Gd-HPDO3A	*	2.91830·10^9	2.58620·10^9
Gd-DTPA - Dimer of Gd-HPDO3A	*	3.32990·10^9	2.31317·10^9
Gd-DTPA - Tetramer of Gd-HPDO3A	*	3.75790·10^9	2.58620·10^9
Gd-BOPTA - Gd-DOTA		3.39895·10^9	2.00326·10^9
Gd-BOPTA - Gd-HPDO3A-NH2		1.16322·10^9	2.1637·10^9
Gd-BOPTA - Gd-HPDO3A	*	2.63829·10^9	2.45349·10^9
Gd-BOPTA - Dimer of Gd-HPDO3A	*	3.04989·10^9	2.1637·10^9
Gd-BOPTA - Tetramer of Gd-HPDO3A	*	3.47789·10^9	2.45349·10^9
Gd-DOTA - Gd-HPDO3A-NH2		8.23328·10^9	2.1637·10^9
Gd-DOTA - Gd-HPDO3A	*	2.98390·10^9	2.45349·10^9
Gd-DOTA - Dimer of Gd-HPDO3A	*	2.71000·10^9	2.1637·10^9
Gd-DOTA - Tetramer of Gd-HPDO3A	*	3.13800·10^9	2.45349·10^9
Gd-HPDO3A-NH2 - Gd-HPDO3A		1.47506·10^9	2.58620·10^9
Gd-HPDO3A-NH2 - Dimer of Gd-HPDO3A		1.88667·10^9	2.31317·10^9
Gd-HPDO3A-NH2 - Tetramer of Gd-HPDO3A		2.31467·10^9	2.58620·10^9
Gd-HPDO3A - Dimer of Gd-HPDO3A		4.11605·10^8	2.58620·10^9
Gd-HPDO3A - Tetramer of Gd-HPDO3A		8.39605·10^8	2.83304·10^9
Dimer of Gd-HPDO3A - Tetramer of Gd-HPDO3A		4.28000·10^8	2.58620·10^9

* denotes a statistically significant difference (p<0.05)

Figure 6. (A) Internalization of different Gd-containing contrast agents into J774A.1 cells. The concentration of Gd complexes in the media is 40 mM. Hypotonic swelling time, 30 min; overall osmolarity of the incubation media, 160 mOsm l^{-1}. (B) Comparison among different cell lines (concentration of Gd–HPDO3A, 100 mM; overall osmolarity, 160 mOsm l^{-1}; incubation time, 30 min). All data in the graphs are reported as mean values ± standard deviation of at least three independent experiments.

Thus, although the hypo-osmotic shock procedure shares with electroporation the fact that both yield a cytoplasmatic localization of the entrapped chemicals, it appears evident that the underlying transient events that yield permeabilization of the cellular membrane may be quite different. One expects that the reorientation of polar heads, upon the application of the electric pulses, will be a much more demanding structural modification with respect to the rearrangements associated with cellular swelling. Our work cannot elucidate the analogies or differences in the permeabilization process that affect membranes with the two procedures. Our aim was limited to testing an additional cell labeling procedure. However, from the attained results, it appears clear that the hypo-osmotic procedure is definitively endowed with lower biological impact than electroporation and it can be strongly recommended for cellular labeling. Table 1 summarizes the pros and cons of pinocytosis, electroporation and hypotonic swelling procedures.

2.4. Characteristics of the Gd Complex and Internalization Efficiency

A study was carried out to assess how the characteristics of the Gd complex may affect the efficiency of the cellular uptake. The following Gd complexes were tested: (A) Gd–DOTA (charge −1); (B) Gd–DTPA (charge −2); (C) Gd–BOPTA (charge −2, with a hydrophobic substituent on the surface of the coordination cage); (D) Gd–HPDO3A (neutral); (E) GdHPDO3A–NH_2 (charge +1); (F) dimer; and (G) tetramer of GdHPDO3A (both neutral) (Scheme 1).

J774A.1 cells were labeled by using the above established conditions (30 min of hypotonic swelling, 160 mOsm l^{-1}, 37 °C). As reported in Fig. 6(A), all the tested compounds were efficiently internalized and the amount of uptaken Gd complexes per cell was distributed over a relatively narrow range (from 2.9×10^9 for Gd–HPDO3A tetramer to 6.6×10^9 for Gd–DTPA). The data were subjected to the Fisher's least significant difference test to account for a better statistical analysis. Only

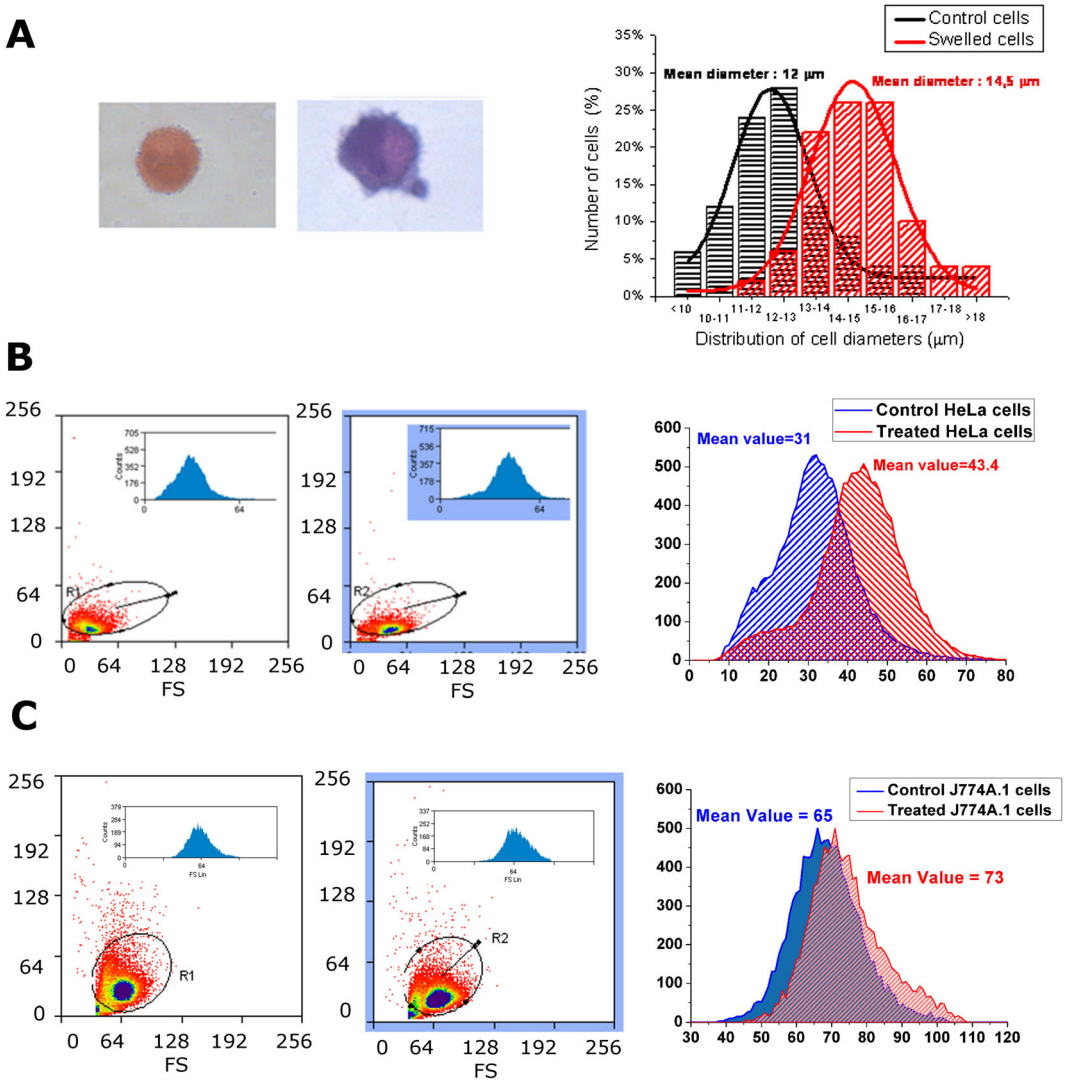

Figure 7. (A) Representative microscopy images of treated (left) and untreated (right) HeLa cells included in low gelling agar and Gaussian distribution of HeLa cell diameters (control cells vs swelled cells) obtained by microscopy. The mean diameter shifts from 12 to 14.5 µm. (B) Cytofluorimetric analysis of control HeLa cells (left) vs treated HeLa cells (right) and comparison between forward scatter distributions. (C) Cytofluorimetric analysis of control j774A.1 cells (left) vs treated j774A.1 cells (right) and comparison between forward scatter distributions.

the uptake of negative Gd complexes was significantly different ($p < 0.05$) from that of the neutral Gd–HPDO3A. In general it seems that charged complexes are more efficiently loaded inside cells than neutral ones, suggesting that electrostatic interactions with charged moieties on the outer cell membranes may have a positive role in the internalization process. However, the observed behavior is somewhat unexpected. One would have expected a passive transit across the leaky membrane, but this does not exactly appear to be the case. The exchange of materials across the membrane in swelled cells appears to be a complex process and an explanation of the observed behavior is not yet available. Comparison between monomer, dimer and tetramer of Gd–HPDO3A suggests that the increase in the molecular size has a rather small effect on the loading efficiency ($p > 0.05$ respect to Gd–HPDO3A).

2.5. Tests on Different Cell Lines

In order to evaluate whether hypotonic swelling methodology can be considered a general cellular labeling route, the herein optimized method (160 mOsm l^{-1}, 100 mM Gd–HPDO3A, 30 min, 37 °C) was applied to other cell lines, namely Igrov-1, B16-F10, U937, 293 T, MDA and HeLa cells. From the results reported in Fig. 6(B) it is evident that the considered cell lines are differently able to internalize Gd–HPDO3A by applying the hypotonic swelling method. However, concerning the task tackled in this work, all tested cell lines showed sufficient loading of MRI probes, invariantly above the threshold for MRI visualization.

2.6. Insights into Cell Morphology Changes Upon Hypotonic Treatment

In order to obtain more insight into the change in the cellular volume upon hypotonic swelling, treated and control cells underwent a microscopic and cytometric analysis. In Fig. 7(A) microscopy images of representative, treated and untreated, HeLa cells, immobilized in low gelling agar, are reported. Hela cells were selected as representative of the other tested cell lines because the increase in cell size upon hypotonic swelling was particularly visible and quantifiable.

The contours of the swelled cells were definitively less regular than the control ones and, often, one or more well defined bump(s) were observed. The occurrence of this feature seemed to anticipate the formation of microvesicles leaving the mother cells. The mean cell diameter of HeLa cells increased from 12 to 14.5 μm upon the application of the hypotonic swelling, as clearly detected from the Gaussian distribution of cell size obtained by optical microscopy.

As previously reported (40) flow cytometric analysis of forward and side scatter provides an indirect observation of cell morphology. In particular, side scatter can be related to the internal complexity of the particles being observed, whereas forward scatter can be related to the cell size. Since forward scatter is proportional to the cell volume, this parameter has been used as an indirect reporter of the cell size distribution. Figure 7(B and C) reports the cytometric results obtained for control and treated HeLa and J774A.1 cells, respectively. A shift in the mean value of forward scatter distribution for treated cells with respect to the one related to untreated cells was clearly detected.

3. CONCLUSIONS

In this work it has been shown that hypotonic swelling represents an efficient and biocompatible method to label cells with paramagnetic Gd complexes. The labeling efficiency depends on many parameters such as incubation time, concentration of the probe in the hypotonic solution, temperature and the characteristics of the molecules.

By applying this methodology the uptaken molecules distribute in the cytoplasm as witnessed by internalizing the fluorescent CarboxyFluorescein. One may expect that the cytoplasmatic compartmentalization results in a higher stability of the internalized molecule as it avoids the most 'aggressive' environment that it would have been met along the endosomes/lysosome internalization pathway (41–43). Moreover this method appears particularly useful for cell lines that are not able to internalize high amounts of molecules by pinocytosis (e.g. K562 cells) and for the internalization of molecules that can be degraded by the 'harsh' microenvironment of the endosomal vesicles.

In summary, hypotonic swelling of cells offers a 'soft' route for MRI cellular labeling. The method has been mainly tested for the internalization of Gd–HPDO3A but it has been shown that other complexes as well as a fluorescent probe (CarboxyFluorescein) can also be loaded efficiently inside cells. In principle one may expect that this methodology will be efficiently used to load other molecular systems inside cells. The comparison among the available techniques for cellular labeling (pinocytosis, electroporation and hypotonic swelling) highlights advantages and disadvantages of the three procedures. The operational simplicity together with the absence of invasiveness may represent undoubtedly a great advantage for the herein reported methodology and its use may open the way to new applications in molecular imaging.

4. EXPERIMENTAL

4.1. Chemicals and Cells

Gd–HPDO3A (ProHance™, Bracco), Gd–BOPTA (MultiHance™, Bracco), Gd–DOTA (Dotarem™, Guerbet) and Gd–DTPA (Magnevist™, Shering) are commercial agents. Gd–HPDO3A-dimer, Gd–HPDO3A-tetramer and Gd–HPDO3A-NH_2 were synthetized in our laboratory (44). All chemicals were purchased from Sigma Chemical Co., St Louis, MO, USA. All cell lines were obtained from American Type Culture Collection (ATCC, Manassas, VA, USA).

J774A.1 (murine macrophages), B16-F10 (murine melanoma) and MDA (murine breast cancer) cells were grown in Dulbecco's modified Eagles's medium (DMEM). U937 (human leukemic monocyte lymphoma), Igrov-1 (human ovarian cancer), 293 T (human embryonic kidney cell), HeLa (human cervical cancer) and K562 (human immortalized myelogenous leukemia) cells were maintained in RPMI 1640 medium. Both the media were supplemented with 10% (v/v) heat-inactivated fetal bovine serum, 100 U/ ml penicillin and 100 mg ml^{-1} streptomycin. DMEM, RPMI, fetal bovine serum, trypsin and penicillin–streptomycin mixture were purchased from Lonza, (Lonza Sales AG, Verviers, Belgium).

Cells were seeded in 75 cm^2 flasks at density of ca. 2×10^4cells cm^{-2} in a humidified 5% CO_2 incubator at 37 °C. When J774A.1 cells reached confluence, they were detached by means of a scraper. The other cell types were detached by

using a mixture of trypsin and EDTA. All the used cells were negative for mycoplasma as tested by using MycoAlert™ Mycoplasma Detection Kit by Lonza (Lonza Sales AG, Verviers, Belgium).

4.2. Loading of GdHPDO3A by Hypotonic Swelling

Cells were placed in a hypotonic solution containing the contrast agent to be loaded (PBS solution with a variable concentration of NaCl defined by the wanted osmolarity, ranging from 130 to 200 mOsm l^{-1}). Then the cells were incubated at 37 °C for a time ranging from 15 to 120 min. The concentration of Gd–HPDO3A in the hypotonic solution ranged from 0 (control) to 100 mM. After the incubation time the physiological morphology of cells was restored by changing the osmolarity of the external solution to an isotonic condition (280 mOsm l^{-1}) through the addition of a proper concentration of phosphate buffer saline for 15–30 min. After this treatment the samples were extensively washed by using PBS to remove the non-internalized Gd-containing molecules. The osmolarity of the used solutions have been monitored by using a manual Löser type 6 Micro-Osmometer.

4.3. Loading of GdHPDO3A by Electroporation

For electroporation about 3×10^6 J774A.1 or K562 cells were dispersed into 0.8 ml of PBS solution containing different concentrations of Gd–HPDO3A (0–100 mM, osmolarity fixed at 280 mOsm l^{-1} and pH 7.4). Then cells were subjected to electroporation at room temperature using a Bio-Rad Gene Pulser™ provided with a Bio-Rad Capacitance Extender (125–960 μF). The used electroporation protocol relies on standards for mammalian cells given by Bio-Rad, that is, electroporation using an exponential decay protocol with a capacitance of 960 μF, voltage of 0.2 kV, and time constant τ ranging from 12 to 20 ms. After electroporation the cells were cooled with ice for 30 min. Then, the cells were washed three times with PBS, suspended into 50 μl of PBS and used for experiments.

4.4. Loading of GdHPDO3A by Pinocytosis

The procedure used for cell labeling by pinocytosis is the one previously reported by our group (14). About 5×10^5 J774A.1 cells or K562 cells were seeded on 6 cm Petri dishes. After one day, plates were incubated for 5 h (J774A.1) or 18 h (K562) with 3 ml of cell culture medium containing Gd–HPDO3A at different concentrations (0–100 mM). After the incubation, cells were extensively washed, detached and used for the analysis.

4.5. Cellular Labeling with 5(6) CarboxyFluorescein by Hypotonic Swelling

5(6)-CarboxyFluorescein (CF, Sigma Aldrich) has been dissolved in phosphate buffer and internalized into J774A.1 cells using the osmotic swelling methodology (160 mOsm l^{-1}, 30 min, CF in the hypotonic solution at the concentration of 0.5 mM). After labeling, cells were seeded and maintained in the culture medium for 4 h, then extensively washed with PBS and finally fixed with 0.3% paraformaldehyde. Nuclei were marked using Hoechst 33342. Fluorescence images were obtained using Zeiss microscopy (CF: $\lambda_{ex} = 492$ nm, $\lambda_{em} = 517$ nm; Hoechst 33342: $\lambda_{ex} = 350$ nm, $\lambda_{em} = 451$ nm).

4.6. Evaluation of Membrane Resealing After Hypotonic Swelling Labeling

In order to evaluate the resealing time of J774A.1 cells membrane after the application of hypotonic swelling labeling, Methylene Blue staining of cells was carried out. Briefly, J774A.1 cells were subjected to hypotonic swelling for 30 min in the absence of the blue dye. Then the iso-osmotic conditions were restored. At different time points from this step, Methylene Blue dye (2.5 mM) was added to cells for 5 min, then cells were washed and the percentage of Methylene Blue positive cells was evaluated by counting the colored cells. The amount of dye internalized during the last 5 min of the swelling step (i.e. before the resealing step) was taken as starting control.

4.7. Cell Viability and Proliferation Tests

For assessing viability, J774A.1 and K562 cells were counted by means of the Trypan Blue exclusion assay, before and after the labeling procedure (pinocytosis, electroporation or hypotonic swelling) in the presence of Gd–HPDO3A. Experiments in the neat buffer solution were carried out and the results used as control. The procedure allows accurate determination of the cell viability since viable cells do not take up Trypan Blue. Cells were added with 0.4% solution of Trypan Blue in PBS (pH 7.2–7.3; 1:1 v/v) and counted using a hemacytometer. For proliferation ability, the labeled cells were seeded and maintained in the fresh culture medium for different time periods (up to 3 days), then detached and counted excluding dead cells using Trypan Blue. The ratio between the number of cells at each time point and the number of cells at the beginning of the experiment (N/N_0) is reported.

4.8. Evaluation of Cell Apoptosis

J774A.1 cells were double-stained with acridine orange/propidium iodide for assessing apoptotic cells. Cells were loaded with Gd–HPDO3A using pinocytosis, electroporation or hypotonic swelling, as described above, and then plated in 24-well plates. After 24 or 48 h they were extensively washed with PBS and incubated with PBS containing 5 μg ml^{-1} of acridine orange (Sigma Aldrich) and 5 μg ml^{-1} of propidium iodide (Sigma Aldrich) for 5 min. The cells were viewed under fluorescent microscopy, photographed and the colored apoptotic cells were counted.

4.9. Determination of Reactive Oxygen Species Production

Intracellular reactive oxygen species production in J774A.1 cells after the treatment with the selected labeling method was examined by using 2′,7′-dichlorofluorescein diacetate (H2DCFDA) (Invitrogen). Briefly, after labeling with ProHance, cells were incubated with H2DCFDA 5 μM in PBS for 30 min at 37 °C, then washed twice with PBS. The fluorescence signal was measured using a Fluoro-Max4 spectrofluorometer, Horiba Scientific (excitation 493 nm and emission 522 nm). Results are shown as ratio of the fluorescent signal (normalized to the number of cells counted using a hemacytometer) obtained for treated cells over the signal from control cells.

4.10. Quantification of Intracellular Gd^{3+}

At the end of each experiment, labeled cells were lysed by sonication by using a Bandelin Sonoplus Sonicator (20 kHz,

power 30%, 20 s). Then cell lysates were treated with HCl 37% (50:50 v:v) in sealed vials at 120 °C overnight in order to destroy the Gd complexes and obtain Gd^{3+} aqua-ion. The R_1 of these solutions was measured at 21 MHz and 25 °C on a Stelar SpinMaster Relaxometer (Mede, Pavia, Italy) and the Gd^{3+} concentration was calculated using a calibration curve obtained using standard solutions of $GdCl_3$ (45). The total protein content was measured by the Bradford method (46) using bovine serum albumin as standard (1 mg of protein is equal to 4.5×10^6 for K562, 2.5×10^6 for J77A.1, 2.8×10^6 for Igrov-1, 4.3×10^6 for B16-F10, 6.5×10^6 for U937, 2.7×10^6 for HeLa, 1.9×10^6 for MDA, respectively).

4.11. MR Imaging of Gd-Labeled Cell Pellets

For the acquisition of the MR images, cells were detached, extensively washed with PBS and collected in 50 μl of PBS, then transferred into glass capillaries and centrifuged at 1500 rpm for 5 min. The cells-loaded glass capillaries were placed in agar for image acquisition. MR images were acquired at 7.1 T using a Bruker Avance 300 spectrometer equipped with a micro-imaging probe. T_1-Weighted images were acquired using a standard T_1-weighted MSME (multislice multiecho) sequence with the following parameters: repetition time (TR) = 50–250 ms, echo time (TE) = 3.3 s, field of view (FOV) = 1 × 1 cm, slice thickness = 1 mm. T_2-weighted images were acquired using a standard T_2-weighted RARE (rapid acquisition with refocused echoes) sequence with the following parameters: TR = 5000 ms, TE = 5.5 s, FOV = 1 × 1 cm, slice thickness = 1 mm, RARE factor = 4–32 depending on the T_2^* of the sample. T_1 values were measured by using a saturation recovery spin echo sequence: TE = 3.8 ms, 16 variable TR ranging from 50 to 5000 ms, FOV = 1 × 1 cm, slice thickness = 1 mm. T_2 values were measured by using a MSME sequence: TR = 2000 ms, 10 variable TE ranging from 11 to 500 ms, FOV = 1 × 1 cm, slice thickness = 1 mm.

4.12. Assessment of Cell Volume Increase Upon Application of the Hypotonic Treatment.

The assessment of the increase in the cellular size upon hypotonic swelling was carried out on HeLa cells by direct microscopic observation and by cytofluorimetric assay. For the first method cells subjected to hypotonic swelling and control cells were suspended in 2% liquid low gelling agar (kept at 37 °C) at a ratio of 1:1 v/v and then placed at room temperature to allow for the solidification of the gel (that occurs in ca. 10 min). The agar had been previously prepared by dissolving low gelling Agar (Sigma Aldrich) into PBS buffer containing a proper amount of NaCl (final osmolarity of 160 or 280 mOsm l^{-1} for treated or control cells, respectively). After the solidification, cells were embebbed in paraffin, and 2.5 μm de-waxed sections were stained and counterstained with hematoxylin/eosin and observed with an Olympus Bhl-2 microscope equipped with a Leica DFC320 photographic system. The observation of cells was carried out in consecutive slices in order to evaluate for each cell the proper diameter. The measurement was performed for 50 cells and values were fitted using a Gaussian curve. Finally, mean diameter and standard deviation were extrapolated.

In the second experiment cell size variation in response to the labeling treatment was assessed by flow cytometric analysis (36). Briefly, 2×10^5 treated or control cells were suspended in 1 ml of PBS at the proper osmolarity. Flow cytometric analysis was carried out on a CyAn ADP instrument (DakoCytomation) and each sample was analyzed at least twice with 50.000 event counts at a medium flow rate. PMT (Photomultiplier Tube) voltage settings for forward and side scatter were 250 and 300, respectively. Forward and side scatter data qwew collected and their analysis was performed using Summit 4.2 software (DakoCytomation).

Acknowledgements

This work was carried out in the frame of the EU-FP7 integrated project ENCITE. Economic and scientific support from Cost Action TD1004 (Theragnostics Imaging and Therapy), the Italian Minister of Research (grant PRIN 2009235JB7) and the Italian Consortium CIRCMSB are also gratefully acknowledged.

REFERENCES

1. Rodriguez-Porcel M. In vivo imaging and monitoring of transplanted stem cells: clinical applications. Curr Cardiol Rep 2010; 12(1): 51–58.
2. Jacquier A, Higgins CB, Saeed M. MR imaging in assessing cardiovascular interventions and myocardial injury. Contrast Media Mol Imag 2007; 2(1): 1–15.
3. Pathak AP, Gimi B, Glunde K, Ackerstaff E, Artemov D, Bhujwalla ZM. Molecular and functional imaging of cancer: advances in MRI and MRS. Meth Enzymol 2004; 386: 3–60.
4. Modo M, Mellodew K, Cash D, Fraser SE, Meade TJ, Price J, Williams SC. Mapping transplanted stem cell migration after a stroke: a serial, in vivo magnetic resonance imaging study. Neuroimage 2004; 21: 311–317.
5. Himmelreich U, Dresselaers T. Cell labeling and tracking for experimental models using Magnetic Resonance Imaging. Meth 2009; 48: 112–124.
6. Hoehn M, Wiedermann D, Justicia C, Ramos-Cabrer P, Kruttwig K, Farr T, Himmelreich U. Cell tracking using magnetic resonance imaging. J Physiol 2007; 584: 25–30.
7. Bulte JW, Kraitchman DL. Iron oxide MR contrast agents for molecular and cellular imaging. NMR Biomed 2004; 17(7): 484–499.
8. Modo M, Hoehn M, Bulte JW. Cellular MR imaging. Mol Imag 2005; 4(3): 143–164.
9. Herynek V, Berková Z, Dovolilová E, Jirák D, Kříž J, Girman P, Saudek F, Hájek M. Improved detection of pancreatic islets in vivo using double contrast. Contrast Media Mol Imag 2011; 6(4): 308–313.
10. Strijkers GJ, Mulder WJ, van Tilborg GA, Nicolay K. MRI contrast agents: current status and future perspectives. Anticancer Agents Med Chem 2007; 7(3): 291–305.
11. Aime S, Barge A, Cabella C, Crich SG, Gianolio E. Targeting cells with MR imaging probes based on paramagnetic Gd(III) chelates. Curr Pharm Biotechnol 2004; 5(6): 509–518.
12. Aime S, Cabella C, Colombatto S, Geninatti Crich S, Gianolio E, Maggioni F. Insights into the use of paramagnetic Gd(III) complexes in MR-molecular imaging investigations. J Magn Reson Imag 2002; 16(4): 394–406.
13. Geninatti Crich S, Biancone L, Cantaluppi V, Duo D, Esposito G, Russo S, Camussi G, Aime S. Improved route for the visualization of stem cells labeled with a Gd-/Eu-chelate as dual (MRI and fluorescence) agent. Magn Reson Med 2004; 51: 938–944.
14. Terreno E, Geninatti Crich S, Belfiore S, Biancone L, Cabella C, Esposito G, Manazza AD, Aime S. Effect of the intracellular localization of a Gd–based imaging probe on the relaxation enhancement of water protons. Magn Reson Med 2006; 55(3): 491–497.
15. Terreno E, Castelli DD, Aime S. Encoding the frequency dependence in MRI contrast media: the emerging class of CEST agents. Contrast Media Mol Imag 2010; 5(2): 78–98.
16. Ferrauto G, Castelli DD, Terreno E, Aime S. In vivo MRI visualization of different cell populations labeled with PARACEST agents. Magn Reson Med 2013; 69(6): 1703–1711.
17. Aime S, Carrera C, Delli Castelli D, Geninatti Crich S, Terreno E. Tunable imaging of cells labeled with MRI-PARACEST agents. Angew Chem Int Ed Engl 2005; 44(12): 1813–1815.
18. Ahrens ET, Rothbächer U, Jacobs RE, Fraser SE. A model for MRI contrast enhancement using T_1 agents. Proc Natl Acad Sci U S A 1998; 95(15): 8443–8448.

19. Schmalbrock P, Hines JV, Lee SM, Ammar GM, Kwok EW. T_1 measurements in cell cultures: a new tool for characterizing contrast agents at 1.5T. J Magn Reson Imag 2001; 14(5): 636–648.
20. Gianolio E, Stefania R, Di Gregorio E, Aime S. MRI paramagnetic probes for cellular labeling. Eur J Inorg Chem 2012; (12): 1934–1944. DOI:10.1002/ejic.201101399
21. Geninatti Crich S, Barge A, Battistini E, Cabella C, Coluccia S, Longo D, Mainero V, Tarone G, Aime S. Magnetic resonance imaging visualization of targeted cells by the internalization of supramolecular adducts formed between avidin and biotinylated Gd-chelates. J Biol Inorg Chem 2005; 10: 78–86.
22. Kobayashi H, Kawamoto S, Saga T, Sato N, Ishimori T, Konishi J, Ono K, Togashi K, Brechbiel MW. Avidin-dendrimer-(1B4M-Gd) (254): a tumor-targeting therapeutic agent for gadolinium neutron capture therapy of intraperitoneal disseminated tumor which can be monitored by MRI. Bioconj Chem 2001; 12: 587–593.
23. Gianolio E, Arena F, Strijkers GJ, Nicolay K, Högset A, Aime S. Photochemical activation of endosomal escape of MRI-Gd-agents in tumor cells. Magn Reson Med 2011; 65(1): 212–219.
24. Strijkers GJ, Hak S, Kok MB, Springer CS Jr, Nicolay K. Three-compartment T_1 relaxation model for intracellular paramagnetic contrast agents. Magn Reson Med 2009; 61(5): 1049–1058.
25. Kok MB, Hak S, Mulder WJ, van der Schaft DW, Strijkers GJ, Nicolay K. Cellular compartmentalization of internalized paramagnetic liposomes strongly influences both T_1 and T_2 relaxivity. Magn Reson Med 2009; 61(5): 1022–1032.
26. Neumann E, Sowers AE, Jordan CA. Electroporation and Electrofusion in Cell Biology. Plenum: New York, 1989.
27. Ferret E, Evrard C, Foucal A, Gervais P. Volume changes of isolated human K562 leukemia cells induced by electric field pulses. Biotechnol Bioeng 2000; 67(5): 520–528.
28. Teissie J, Eynard N, Gabriel B, Rols MP. Electropermeabilization of cell membranes. Adv Drug Deliv Rev 1999; 35: 3–19.
29. Babiuk S, van Drunen Littel-van den Hurk S, Babiuk LA. Delivery of DNA vaccines using electroporation. Meth Mol Med 2006; 127: 73–82.
30. Joshi RP, Schoenbach KH. Bioelectric effects of intense ultrashort pulses. Crit Rev Biomed Eng 2010; 38(3): 255–304.
31. Sinha B, Koster D, Ruez R, Gonnord P, Bastiani M, Abankwa D, Stan RV, Butler-Browne G, Vedie B, Johannes L, Morone N, Parton RG, Raposo G, Sens P, Lamaze C, Nassoy P. Cells respond to mechanical stress by rapid disassembly of caveolae. Cell 2011; 144: 402–413.
32. Maeda M, Thompson GA. On the mechanism of rapid plasma membrane and chloroplast envelope expansion in Dunaniella Salina exposed to hypoosmotic shock. J Cell Biol 1986; 102: 289–297.
33. D'Alessandro M, Russel D, Morley SM, Davies AM, Lane EB. Keratin mutations of epidermolysis bullosa simplex alter the kinetics of stress response to osmotic shock. J Cell Sci 2002; 115: 4341–4351.
34. Cornet M, Lambert IH, Hoffmann EK. Relation between cytoskeleton, hypo-osmotic treatment and volume regulation in Ehrlich ascites tumor cells. J Membrane Biol 1993; 131: 55–66.
35. Marian T, Krasznai Z, Balkay L, Balazs M, Emri M, Bene L, Tron L. Hypo-osmotic shock induces an osmolality-dependent permeabilization and structural changes in the membrane of carp sperm. J Histochem Cytochem 1993; 41: 291–297.
36. Rossi L, Serafini S, Pierigé F, Antonelli A, Cerasi A, Fraternale A, Chiarantini L, Magnani M. Erythrocyte-based drug delivery. Expert Opin Drug Deliv 2005; 2(2): 311–322.
37. Markov DE, Boeve H, Gleich B, Borgert J, Antonelli A, Sfara C, Magnani M. Human erythrocytes as nanoparticle carriers for magnetic particle imaging. Phys Med Biol 2010; 55(21): 6461–73.
38. Antonelli A, Sfara C, Mosca L, Manuali E, Magnani M. New biomimetic constructs for improved in vivo circulation of superparamagnetic nanoparticles. J Nanosci Nanotechnol 2008; 8(5): 2270–2278.
39. Kravtzoff R, Urvoas E, Chambon C, Ropars C. Gd–DOTA loaded intored blood cells, a new magnetic resonance imaging contrast agents for vascular system. Adv Exp Med Biol 1992; 326: 347–354.
40. Kiehl T R, Shen D, Khattak S, Jian Li Z, Sharfstein S T. Observations of cell size dynamics under osmotic stress. Cytometry 2011; 79A: 560–569.
41. Huotari J, Helenius A. Endosome maturation. EMBO J 2011; 30(17): 3481–3500.
42. Clague MJ. Molecular aspects of the endocytic pathway. Biochem J 1998; 336(Pt 2): 271–282.
43. Di Gregorio E, Gianolio E, Stefania R, Barutello G, Digilio G, Aime S. On the fate of MRI Gd-based contrast agents in cells. evidence for extensive degradation of linear complexes upon endosomal internalization. Anal Chem 2013; 85(12): 5627–5631.
44. Aime S, Delli castelli D, Terreno E, Fedeli F, Longo DL, Uggeri F. Cest systems exhibiting a concentration indipendent responsiveness. Patent number EP10190161, 2010. Applicant: Bracco Imaging S.p.A.
45. Cabella C, Crich SG, Corpillo D, Barge A, Ghirelli C, Bruno E, Lorusso V, Uggeri F, Aime S. Cellular labeling with Gd(III) chelates: only high thermodynamic stabilities prevent the cells acting as 'sponges' of Gd3+ ions. Contrast Media Mol Imag 2006; 1(1): 23–29.
46. Bradford MM. Rapid and sensitive method for the quantitation of microgram quantities of protein utilizing the principle of protein-dye binding. Anal Biochem 1976; 72: 248–254.

SUPPORTING INFORMATION

Additional supporting information may be found in the online version of this article at the publisher's web site.